

COMPENSATING FOR THE EFFECTS OF REFRACTION IN PHOTOGRAMMETRIC METROLOGY

Stephen Kyle, Stuart Robson, Lindsay MacDonald, University College London, UK
Mark Shortis, RMIT University, Melbourne, Australia

Abstract

As part of the recently completed LUMINAR project, lead by the UK's National Physical Laboratory (NPL), the 3DIMPact group at University College London (UCL) was given the task of evaluating and correcting the effects of refraction on photogrammetric metrology applications.

Refraction causes light rays to bend. This results in pointing errors which potentially can be corrected. Simulations suggest that the effects over short ranges are small, and possibly negligible, but could be significant over longer ranges, e.g. 10m - 30m. These are certainly found in application areas such as aircraft assembly and therefore deserve attention.

Refraction errors are dominated by thermal changes in the atmosphere. They have been evaluated in some detail in geodesy, and to a much lesser extent in photogrammetry. General atmospheric refraction in metrology applications has not been investigated in detail before, using either photogrammetry or laser trackers.

This paper summarizes the work in the LUMINAR project and outlines its further potential application in an ongoing, parallel project, the Light-Controlled Factory, lead by the University of Bath. Currently a level of correction seems achievable if real-time temperature sensing in the local measurement environment is possible. Here the authors would like to engage with the IWAA to identify potential applications in accelerator alignment.

BACKGROUND

Refraction in a factory environment, primarily due to temperature differences in the air, can cause light rays to bend significantly, particularly over longer ranges. For photogrammetric and laser tracker measurements this means that the locations of targets and reflectors are apparently shifted from their actual positions. If significant, refraction analysis is needed to find ways of modelling and mitigating this error.

As an example, a small linear vertical temperature gradient of approximately 0.5°C per m would cause an apparent target deflection of just under 50µm on an approximately horizontal ray over 10m. Over 30m the apparent shift would be around 0.4mm. If there is a more significant change from floor (colder) to ceiling (warmer) of, say, 10°C over a 6m height change, then at 15m range the shift is around 0.2mm. This is still significant and the scenario could be an aerospace assembly hall.

There is little photogrammetric literature on general atmospheric effects of refraction. There is nothing recent and nothing applicable to industrial environments. Fraser [1] gives an example of work on rock wall movement. Multi-media photogrammetry is, of course, relatively well researched but this deals with refraction at specific surfaces. Maas [2] analyses a conventional situation with an object in water, a camera in air and a plane glass interface between the media. More recently, Muslow [3] handles a more complex arrangement of surfaces.

It is in geodesy that general atmospheric refraction has been handled in most detail. This work demonstrates that by making pointings using two frequencies of light it is possible to correct the refraction error. This requires the measurement of the dispersion (difference in refraction) between red and blue light. For the wavelengths of light normally used in this 2-colour work, the dispersion is 42 times smaller than the refraction angles. Dispersion measurement, and hence refraction correction, are therefore challenging but have been successful. Much early work was done by Williams [4] at the UK's National Physical Laboratory (NPL).

Huiser and Gächter [5] at commercial systems manufacturer Wild Leitz AG (now Leica Geosystems which is part of Hexagon MI) successfully built a working dispersometer for refraction correction at ranges of 100m. For a more recent overview of methods of dealing with refraction and turbulence, see Ingensand [6].

To put the challenge for geodesists in photogrammetric terms, the simulated apparent shifts in object space of red and blue targets at 15m horizontal distance and a 6m height difference with a 10°C linear vertical temperature change, show a difference of only around 5µm. Detecting this level of dispersion at 15m range reliably in a camera is extremely challenging.

In order to evaluate refraction, and apply compensation if possible, 3 approaches have been considered:

- Developing photogrammetric sensor technology to permit dual wavelength correction
- Using the multi-ray intersections typical of multi-camera measurement networks to extract refractive index corrections
- Sensing the environment to determine the 3D variation in refractive index and calculating the error for every ray

Briefly, sensor technology is a challenge not resolved here but future options have been identified. Extracting the

refraction from multi-ray intersection geometry is very difficult when the apparent shift of a target is at the level of the uncertainty in the image measurement. Here the least-squares network solution tends to absorb refraction errors in other network parameters.

The best option currently is to sense the environment, determine refractive index changes and model individual ray refraction errors which can then be removed.

SIMULATION

Using MathCAD as a simulation tool, a ray between target and instrument (camera or laser tracker) is split into segments. In an iterative procedure, the directions of these separate segments are calculated sequentially using the refractive index, and refractive index gradient, corresponding to the local environmental conditions at the current segment position. Figure 1 shows a sample output.

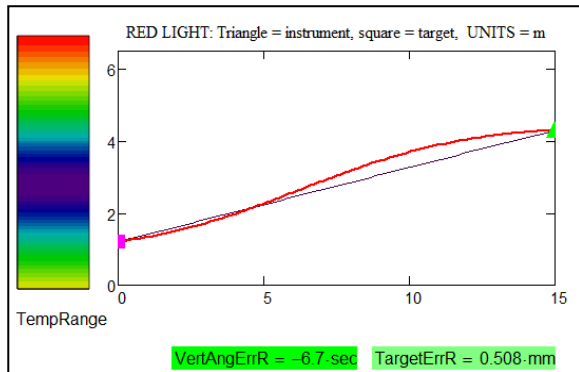


Figure 1 A refracted ray calculation in MathCAD (bending exaggerated for illustration)

The refractive index of air depends on temperature, pressure and humidity, although temperature has the most significant effect. For convenience, the MathCAD simulations assume dry air at a standard pressure of 1013mb and only analyse the effect of an environment defined by varying temperatures. To convert from temperature to refractive index, a well-known equation by Edlén [7] was used in Williams' work [4] but a more recent update by Bönsch and Potulski [8] has been used in the UCL work.

In developing the simulation, the starting point was a simple model of horizontal temperature layers with the ray being traced through the layers using Snell's Law, as illustrated in Figure 2.

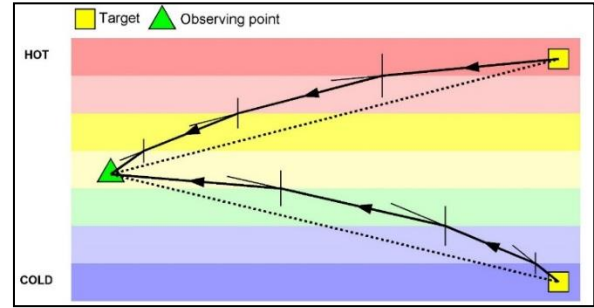
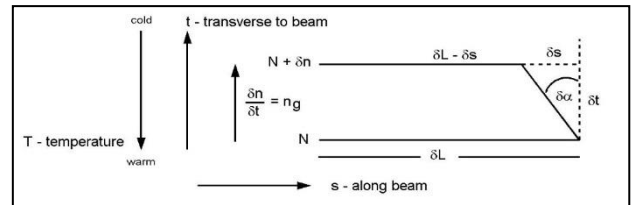


Figure 2 Horizontal temperature layers and refraction modelled by Snell's Law

This has disadvantages. For example, a horizontal ray between a target and instrument at the same height shows no refraction due to bending because the single layer through which the ray travels has a uniform temperature. In practice there is a continuous vertical temperature gradient in this simple case. Modelling was therefore changed to use a differential bending formulation by Williams [4] in order to calculate the curvature of the beam as it propagates, see Figure 3.



$$\delta\alpha = \frac{\delta L}{N} \cdot n_g$$

Figure 3 Modelling formulation due to Williams [4]

Note that Williams' formulation requires the refractive index gradient transverse to the beam, which in general is the appropriate component of the actual refractive index gradient. Applying this to horizontal temperature layers gives very close agreement with the same model using Snell's Law.

In order to allow for a more complex distribution of temperatures in the measurement space, cuboidal voxels now define the simulated atmosphere using 8 temperature values at their corners. Trilinear interpolation of the corner temperatures is used to calculate the temperature at any point within the voxel where ray bending is to be modelled. This can now take place in any direction.

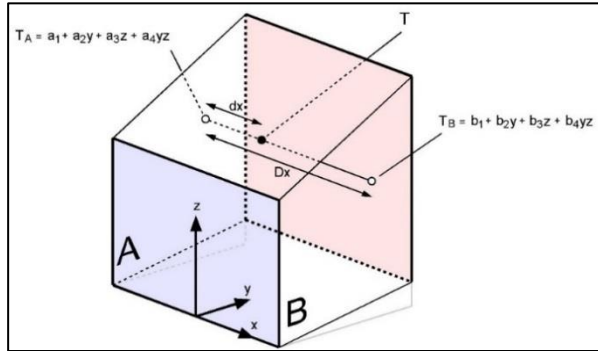


Figure 4 Cuboidal voxels

Figure 4 illustrates trilinear temperature interpolation which is bilinear on two faces of the voxel (T_A , T_B), followed by linear interpolation between the faces to give a final temperature value at the point of interest. The interpolated value of temperature T has the form:

$$T = k_1 + k_2 \cdot x + k_3 \cdot y + k_4 \cdot z + k_5 \cdot x \cdot y + k_6 \cdot y \cdot z + k_7 \cdot z \cdot x + k_8 \cdot x \cdot y \cdot z$$

(The constants $k_1 \dots k_8$ are obtained from the 8 equations given by the 8 temperatures at the 8 known voxel corners.)

This can then be substituted into Bönsch and Potulski's formula [8] to obtain the refractive index, N . The refractive index gradient with respect to the spatial axes can be derived from the spatial temperature gradient (differentiation of the formula above) and the gradient of N with respect to T , again using Bönsch and Potulski's formula. Once the refractive index, and the component of its spatial gradient transverse to the beam are known, Williams' formulation [4] can be used to calculate the bending of the beam.

This analysis applies to 3D space so the movement of the beam in any direction, according to temperature distribution, can be calculated. Again this development stage was checked against the previous one by defining voxel corner temperatures corresponding to a simple layer model. Again agreement was very close.

A final computational check on model validity is a comparison with 2-colour correction in geodesy. These have typically used red and blue wavelengths of 460nm and 230nm respectively. In simulations, the dispersion has a value 42 times smaller than the refraction error angle, which is the value established geodetically. (This applies whether or not a refracted ray follows a simple or complex curve.)

Although pressure and humidity have not been included as variables in determining refractive index, these are already defined in the functional relationship and so would be easy to add. However, an untested assumption remains in that bilinear and trilinear interpolation of temperature is assumed to be valid.

EXPERIMENTAL EVALUATION

In order to relate simulation to practice, a significant amount of experimental work has been done using "boresight" imaging of multi-coloured LED target clusters. Here, long focal length lenses with their narrow viewing angle are ideally suited to imaging distant flat targets and maximising the angular sensitivity attainable from low cost imaging sensors.

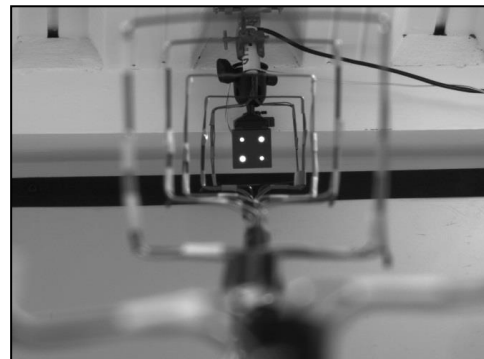
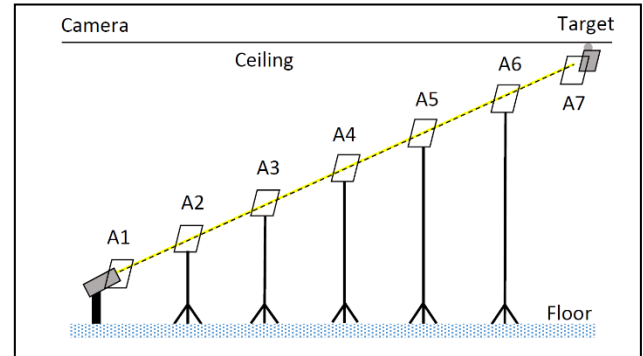


Figure 5 Boresight imaging through "Quad" temperature sensors

In the most recent tests, high quality Kern telephoto lenses of 75mm and 150mm focal length were used to image the target clusters through an array of temperature sensors which form a measurement "duct" between cameras and targets. Figure 5 (top) shows diagrammatically clusters of "quad" temperature sensors, which are four thermocouples on a simple frame. These are arranged to form a viewing duct from a camera on the ground to a cluster of four LED targets in a raised position, and the lower image shows the corresponding camera view.

By manipulating the heating arrangements it was possible, in tests at UCL and on a site provided by project partner Airbus UK, to create different thermal distributions between camera and targets and hence different image shifts due to refraction. Successive pairs of quad targets correspond to the geometry of the cuboidal voxels defined above for the simulation of 3D ray bending, so providing a basis for comparison between simulation and experiment.

Since it is difficult in practice to establish a reference state of zero refraction, and hence measure absolute shifts due to refraction, it is necessary to compare differential image shifts between two thermal states with the corresponding differences from a simulation of the situation.

Whilst a wealth of data have been collected, results from testing using a single camera and target are inconclusive. The camera combination of telephoto lens and uEye imaging chip is itself subject to distortion caused, for example, by thermal warm-up and the way the camera is mounted [9]. It is not a simple matter to separate the effects of image movement due to refraction of the measurement ray and internal movements of the camera itself.

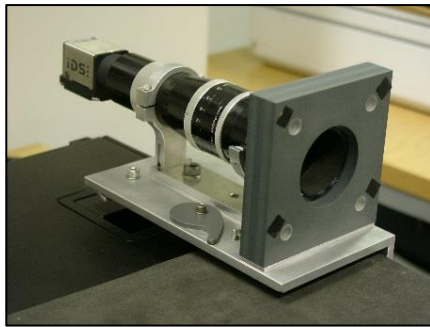


Figure 6 Camera/target module for tests at Airbus UK

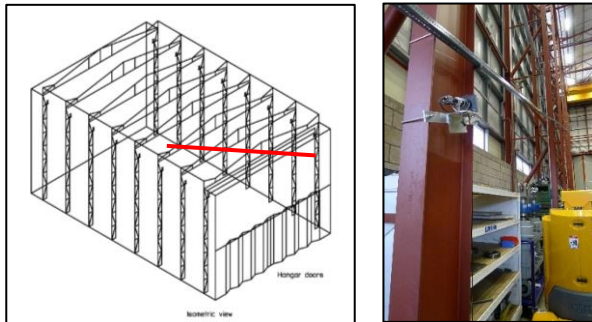


Figure 7 Site location for tests at Airbus UK

In the most recent tests at Airbus, the system has been extended utilising two cameras with LED targets around their lenses to provide a mutually pointing camera/target configuration, see Figure 6. Each occupies one end of a 40m long measurement duct and images the targets around the other camera lens. Figure 7 (left) shows diagrammatically the measurement duct (red) along one wall of a hangar. Figure 7 (right) shows the actual situation.

In this arrangement, the idea is that image shifts due to refraction will be correlated in the views of each camera, whereas shifts due to individual camera movements will not. Preliminary evaluation of the data collected over a one week period, with a range of environmental changes due to natural and building heating, demonstrate significant movements in the imaged target locations. Evaluations are on-going to connect the physically observed changes with the mathematical model.

APPLICATION IN THE LIGHT-CONTROLLED FACTORY PROJECT

In the on-going Light-Controlled Factory (LCF) project [10], the photogrammetric task is to develop a factory-wide network of low-cost cameras capable of tracking and aligning multiple objects and components to a high accuracy in 7 degrees of freedom (7DoF). 7DoF implies continuous monitoring of an object's 6DoF (3D position and angular orientation) over time.

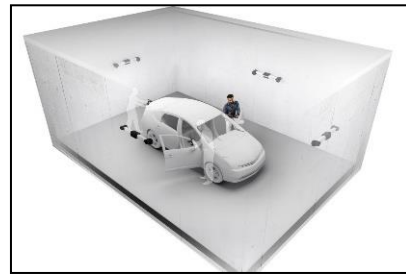


Figure 8 Commercial multi-camera networks from Creaform (top) and Aicon (bottom)

Multi-camera networks are already in commercial use and Figure 8 shows examples from Creaform (now part of Ametek) and Aicon (now part of Hexagon MI). However, they are not yet employed across very large spaces and to achieve that with high levels of accuracy, the UCL team must look at ways of improving the sensitivity.

One method evaluated in some detail has been to improve the calibration of the cameras. Provided a camera is stable, a more accurate mathematical model will improve the accuracy of the pointings from the image to the corresponding target locations of interest.

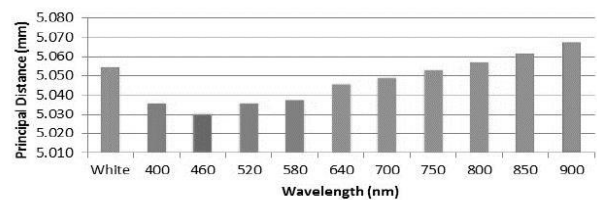


Figure 9 Variation of a camera's principal distance with illumination wavelength

As an example of potential improvement, Figure 9 shows how a camera's principal distance (PD) varies with the illumination wavelength. PD is approximately the focal length at infinity focus and any error in PD will directly affect the measured directions from the camera to the targets. Conventional white-light illumination is a blend of wavelengths and it would be more accurate to use a single illumination wavelength with a well-defined PD applicable to that wavelength only.

Clearly it would also help to mitigate pointing errors due to the measurement environment, specifically refraction errors caused by temperature variations. Given the LCF concept of multiple cameras generating multiple ray intersections to target points of interest, a possible solution might be to determine the refraction errors as part of the bundle adjustment used to analyse the camera and target positions in the network. A bundle adjustment is a commonly used, least-squares optimization of all the camera and target positions in a given measurement configuration

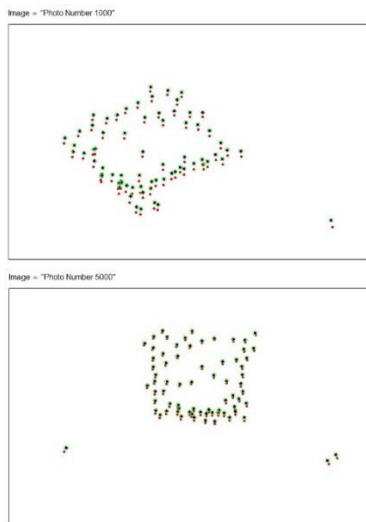


Figure 10 Simulated images in MathCAD of a set of 3D targets

To help evaluate the feasibility of this idea, measurement configurations were simulated, both with and without refraction present. The objective was to see if a comparison of results clearly showed errors due to refraction. Then it might be possible to find ways of filtering out refraction when the only measurements available are those containing possible refraction errors.

Figure 10 shows two simulated images from an example configuration. Here 8 cameras at the same height imaged, at a lower level, around 70 targets with a 3D spread of locations. This was a scaled-up version of a real, small-scale configuration used in the lab. To create significant refraction errors, the height variation from lowest targets to cameras was set to around 30m, with a linear vertical temperature change over this height of some 60°C. In the simulated images un-refracted image locations are black

dots with green circles and refracted positions are red dots, shown with an exaggerated refraction offset to aid visualization. As can be seen, the size of the refracted image offsets depend on relative camera and target location, demonstrated by the comparison of oblique and frontal camera views.

Due to the nature of the least squares estimation process, refraction errors tend to be absorbed into a combination of the disturbed camera and target positions compared with an un-refracted network. This happens to a greater extent when simulated random image measurement error is added to the evaluation. It is yet further complicated when a more irregular thermal distribution is applied. Work is continuing to provide greater constraint within the network adjustment process in conjunction with the thermal model.

At present therefore, the best option for applying refraction correction is to sample physically the temperatures in the measurement space. An initial bundle adjustment will then determine camera and target locations which are close to the actual values. Those can then be used to calculate refracted rays and estimate the apparent target shifts for each ray. That enables the error to be removed. The correction process can, of course, be iterated if required.

POTENTIAL FURTHER WORK

There are a number of options for further evaluating the mitigation of refraction errors:

1. Investigating alternative imaging techniques which may be more sensitive to dispersion measurement and hence directly capable of eliminating refraction errors.
2. Verifying simulation against laser tracker measurements.

By replacing a camera by a laser tracker, for which refraction correction is also important, the issue of instrument deformation confusing the results might be more easily eliminated.

3. Implementing the MathCAD simulations in MatLAB for use in online refraction correction with environmental sensing.

MathCAD is a good tool for developing and documenting mathematical simulation methods, MatLAB is a good tool for online processing of data.

4. Confirming the validity of a simple interpolation method for calculating values between environmental sensors, typically a 3D network of thermal sensors.

5. Evaluating techniques for remotely sensing temperatures in a 3D work space and so avoid the need for physical sensing.

Physically positioned sensors may be an inconvenient addition to the workspace.

6. Investigating other areas, such as accelerator alignment, where refraction correction could be applied.

CONCLUSION

Where refraction effects are significant, correction can be applied in applications where a 3D network of sensors can generate a snapshot of the temperature distribution. Provided that the interpolation of temperatures between sensing nodes is reliable, this enables the calculation of refractive index, and refractive index gradient, along photogrammetric and laser tracking measurement lines of sight. These values in turn enable the error of an apparent target shift to be removed to a significant extent.

ACKNOWLEDGMENT

This work was funded through the EU EMRP LUMINAR project. The EMRP is jointly funded by the EMRP participating countries within the EURAMET and the European Union. The investigation was supported by EPSRC grant EP/K018124/1 'The Light Controlled Factory'

REFERENCES

- [1] C. S. Fraser, "Atmospheric refraction correction in terrestrial photogrammetry," *Photogrammetric Engineering and Remote Sensing*, vol. 45, no. 9, p. 1281 – 1288, Sept. 1979.
- [2] H.-G. Maas, "New developments in multi-media photogrammetry," *Optical 3D measuring techniques III*, 1995.
- [3] C. Muslow, "A flexible multi-media bundle approach," *ISPRS Commission V Symposium*, vol. XXXVIII, no. 5, 2010.
- [4] D. C. Williams, "First field tests of an angular dual-wavelength instrument," *Symposium on Electromagnetic Distance Measurement and the Influence of Atmospheric Refraction*, May 1977.
- [5] A. M. J. Huiser and B. F. Gächter, "A solution to atmospherically induced problems in very high-accuracy alignment and levelling," *Journal of Physics D: Applied Physics*, vol. 22, p. 1630 – 1638, 1989.
- [6] H. Ingensand, "Concepts and solutions to overcome the refraction problem in terrestrial precision measurement," *Geodezija ir Kartografija / Geodesy and Cartography*, vol. 34 (2), p. 61 – 65, 2008.
- [7] B. Edlén, "The refractive index of air," *Metrologia*, vol. 2 (2), p. 71, 1966.
- [8] G. Bönsch and E. Potulski, "Metrologia," vol. 35, pp. 133-139, 1998.
- [9] S. Robson, L. MacDonald, S. Kyle and M. Shortis, "Close range calibration of long focal length lenses in a changing environment," *ISPRS - International Archives of the Photogrammetry, Remote Sensing and Spatial Information Sciences*, Vols. XLI-B5, pp. 115-122, 2016.
- [10] S. Robson, L. MacDonald, S. Kyle, J. Boehm and M. Shortis, "Optimized multi-camera systems for dimensional control in factory environments," *Proceedings of the Institution of Mechanical Engineers, Part B: Journal of Engineering Manufacture*, 2016.